

# Alleviating the $H_0$ and $\sigma_8$ anomalies with a decaying dark matter model

Kanhaiya L. Pandey,<sup>a</sup> Tanvi Karwal<sup>b</sup> and Subinoy Das<sup>a</sup>

<sup>a</sup>Indian Institute of Astrophysics,

Sarjapura Road, 2nd Block Koramangala, Bengaluru, Karnataka – 560034, India

<sup>b</sup>Department of Physics and Astronomy, Johns Hopkins University,

3400 N. Charles St., Baltimore, Maryland – 21218, United States

E-mail: [kanhaiya.pandey@iiap.res.in](mailto:kanhaiya.pandey@iiap.res.in), [tkarwal@jhu.edu](mailto:tkarwal@jhu.edu), [subinoy@iiap.res.in](mailto:subinoy@iiap.res.in)

**Abstract.** The Hubble tension between the  $\Lambda$ CDM-model-dependent prediction of the current expansion rate  $H_0$  using Planck data and direct, model-independent measurements in the local universe from the SH0ES collaboration disagree at  $> 3.5\sigma$ . Moreover, there exists a milder  $\sim 2\sigma$  tension between similar predictions for the amplitude  $S_8$  of matter fluctuations and its measurement in the local universe. As explanations relying on unresolved systematics have not been found, theorists have been exploring explanations for these anomalies that modify the cosmological model, altering early-universe-based predictions for these parameters. However, new cosmological models that attempt to resolve one tension often worsen the other. In this paper, we investigate a decaying dark matter (DDM) model as a solution to both tensions simultaneously. Here, a fraction of dark matter density decays into dark radiation. The decay rate  $\Gamma$  is proportional to the Hubble rate  $H$  through the constant  $\alpha_{\text{dr}}$ , the only additional parameter of this model. Then, this model deviates most from  $\Lambda$ CDM in the early universe, with  $\alpha_{\text{dr}}$  being positively correlated with  $H_0$  and negatively with  $S_8$ . Hence, increasing  $\alpha_{\text{dr}}$  (and allowing dark matter to decay in this way) can then diminish both tensions simultaneously. We find that this secret interaction, if present in the dark sector, can alleviate both tensions and slightly improve the fit to data. The tensions are reduced to  $\sim 1.5\sigma$  for  $H_0$  and  $0.3\sigma$  for  $S_8$  when only considering Planck CMB data and the local SH0ES prior on  $H_0$ . However, the addition of intermediate-redshift data (the JLA supernova dataset and baryon acoustic oscillation data) weakens the effectiveness of this model, bringing the tensions back up to  $\sim 2.5\sigma$  and  $\sim 1.5\sigma$  respectively.

---

## Contents

<b>1</b>	<b>Introduction</b>	<b>2</b>
<b>2</b>	<b>Decaying dark matter model</b>	<b>3</b>
2.1	Background dynamics	3
2.2	Calculation of $\Delta N_{\text{eff}}$	4
2.3	Effects on observables	4
<b>3</b>	<b>Methodology</b>	<b>6</b>
<b>4</b>	<b>Results</b>	<b>7</b>
<b>5</b>	<b>Discussion and conclusions</b>	<b>13</b>

---

## 1 Introduction

The simple  $\Lambda$ CDM concordance model has been immensely successful in describing numerous cosmological observables at different epochs [1–3]. Nonetheless, when fit to measurements of the early universe, the  $\Lambda$ CDM model finds results inconsistent with observations of the late universe [4]. These include the persistent Hubble tension [5] as well as the milder  $S_8$  tension [6].

The current state-of-the-art experiment Planck which measures the cosmic microwave background (CMB) radiation, assumes a flat  $\Lambda$ CDM model to extract cosmological parameter values and finds the local expansion rate  $H_0$  to be  $67.37 \pm 0.54$  km/s/Mpc [7]. On the other hand, the SH0ES collaboration finds the larger value  $H_0 = 73.52 \pm 1.62$  km/s/Mpc [8, henceforth R18] through model-independent measurements of the local universe, at  $\gtrsim 3.5\sigma$  tension with the Planck value. This tension between the early and late universe exists even without Planck CMB data or the SH0ES distance ladder [4]. Another direct measurement of  $H_0 = 71.9^{+2.4}_{-3.0}$  km/s/Mpc [9] from the H0LiCOW collaboration based on lensing time delays is in moderate tension with Planck, while a constraint from Big Bang nucleosynthesis (BBN) combined with baryon acoustic oscillation (BAO) data of  $H_0 = 66.98 \pm 1.18$  km/s/Mpc [4] is inconsistent with SH0ES.

There is also evidence of  $\gtrsim 2\sigma$  tension between the constraints from Planck on the matter density  $\Omega_m$  and the amplitude  $\sigma_8$  of matter fluctuations in linear theory and those from local measurements [6, 10]. Planck derives  $S_8 = \sigma_8(\Omega_m/0.3)^{0.5} = 0.832 \pm 0.013$  whereas local measurements find the smaller  $S_8^{SZ} = \sigma_8(\Omega_m/0.27)^{0.3} = 0.78 \pm 0.01$  from Sunyaev-Zeldovich cluster counts [11] and  $S_8 = 0.783^{+0.021}_{-0.025}$  from the DES weak-lensing surveys [12].

Although systematic causes for these discrepancies cannot entirely be ruled out, numerous potential systematics have been investigated and exonerated over the years while the tensions have persisted and worsened [7, 10, 13–18]. Hence, we must consider the alternative - that the model-dependent results from the early universe are inconsistent with the model-independent measurements of the late universe because the  $\Lambda$ CDM model of cosmology is incorrect.

There have been numerous attempts at resolving these discrepancies via non-standard cosmological models [19–28, and references therein], however, most such attempts at solving the Hubble tension worsen the  $S_8$  tension and vice-versa. Solutions of the Hubble tension must resolve the tension by reducing the size  $r_s$  of the sound horizon to remain consistent with data [29–31]. This requires a modification of early-universe physics [19, 20]. On the other hand, a solution to the  $S_8$  tension would require late-universe physics that leads to a suppression of the linear matter power spectrum.

In this paper, we tackle both requirements with a decaying dark matter (DDM) model. In this scenario, a fraction of dark matter density decays into dark radiation per Hubble time [32], with the effect being amplified close to the onset of matter domination. This leads to an increase in the expansion rate relative to  $\Lambda$ CDM around recombination, resulting in a decrease in  $r_s$ . Fits to the CMB then predict a higher  $H_0$ , alleviating the Hubble tension. Moreover, dark matter decaying into dark radiation suppresses structure formation at large scales, leading to smaller  $S_8$  values. This model can hence simultaneously diminish both the Hubble and the  $S_8$  tensions. Testing against various cosmological datasets, we find that this DDM model can provide a better fit to some datasets and simultaneously alleviate the two aforementioned tensions, but not fully resolve them. We also find that at most, a fraction  $f_{\text{dm}} \lesssim 0.003$  of dark matter can decay into dark radiation in the light of recent Planck, supernova and BAO data, and an external prior on  $H_0$  from R18. This paper is organised as follows. A brief description of the model is given in Section 2, along with its effect on observables. In Section 3, we provide a detailed description of our analysis. Our results are presented in Section 4 and discussed in Section 5 where we also conclude.

## 2 Decaying dark matter model

Motivation for exploring a DDM resolution to the Hubble tension comes from considering the effective radiation degrees of freedom  $N_{\text{eff}}$  [2, 7, 22]. Increasing the amount of radiation in the early universe such that  $\Delta N_{\text{eff}} \sim 0.4 - 1$  has been shown to diminish the Hubble tension [2]. This extra radiation must be ‘dark’ as the presence of an extra photon-like component is strongly constrained by both BBN and the CMB [33]. A fourth, massive, sterile neutrino could provide such extra dark radiation however, the existence of such a particle is constrained by oscillation experiments [34].

The scenario explored here follows the model proposed by Ref. [32]. It involves dark radiation interacting within the dark sector, in particular, a particle (beyond the framework of the standard model) decaying into an extra dark radiation component. All the dark radiation in this scenario is a product of dark matter decay and forms a small fraction of the total dark matter density. The decay rate  $\Gamma$  determines this fraction  $f_{\text{dm}}$  of dark matter energy density that decays into dark radiation. This fraction remains nearly constant over time after matter-radiation equality. If  $f_{\text{dm}}$  is large, it can alter the expansion rate as shown in Fig. 1, which we demonstrate leads to a higher predicted  $H_0$ . Moreover, the decay naturally reduces the amount of dark matter in galaxies and clusters leading to smaller predicted values of  $S_8$ . A brief description of the background dynamics of the model, contribution of dark radiation to  $N_{\text{eff}}$  and effect on observables is discussed in the following subsections.

### 2.1 Background dynamics

A general coupling between dark matter and dark radiation can be described by the energy balance equations [35]

$$\dot{\rho}_{\text{dm}} + 3H\rho_{\text{dm}} = -Q \quad (2.1)$$

$$\dot{\rho}_{\text{dr}} + 3H(1 + w_{\text{dr}})\rho_{\text{dr}} = Q \quad (2.2)$$

where  $\rho_{\text{dm}}$  and  $\rho_{\text{dr}}$  are the dark matter and dark radiation energy densities and  $H = \dot{a}/a$  is the Hubble rate, where  $a$  is the scale factor and overdots denote derivatives with respect to conformal time. We also assume dark radiation has an equation of state  $w_{\text{dr}} = P_{\text{dr}}/\rho_{\text{dr}} = 1/3$ . A positive rate of energy transfer  $Q$  denotes the direction of energy transfer from dark matter to dark radiation. Non-zero values of  $Q$  imply that dark matter no longer redshifts exactly as  $a^{-3}$  nor dark radiation as  $a^{-4}$ . We adopt the covariant form of the energy-momentum transfer 4-vector introduced in [35]

$$Q = \Gamma\rho_{\text{dm}}, \quad (2.3)$$

where the exact form of the interaction rate  $\Gamma$  depends on the details of the particle physics of the decay process.

Many forms of  $\Gamma$  have been studied in the literature [27, 36–39]. Here, we explore the simple case where  $\Gamma = \alpha H$ , where  $\alpha$  is a constant and  $H$  is the Hubble rate. Although we do not model the particle physics resulting in  $\Gamma \propto H$ , we refer the reader to two fundamental particle physics motivations for such an interaction. As discussed in Section 5 of Ref. [32], if dark matter is a coherently oscillating scalar field and decays into light fermions similar to the reheating mechanism, it can give rise to our DDM set up. It may also arise in the model proposed by Ref. [40], where a fraction of dark matter converts to dark radiation through late kinetic decoupling and Sommerfeld-enhanced dark matter annihilation. The mass ranges for dark matter particles in each of these models differ greatly. As our analysis here is phenomenological, our constraints are independent of the mass of the dark matter particle undergoing decay. Interpreting these results in the framework of a particular fundamental model can translate our constraints to particle mass and interaction cross-section.

For  $\Gamma = \alpha H$ , the background evolution is readily solved

$$\rho_{\text{dm}} = \rho_{\text{dm},0} a^{-(3+\alpha_{\text{dr}})} \quad (2.4)$$

$$\rho_{\text{dr}} = \rho_{\text{dr},0} a^{-3(1+w_{\text{dr}})} + \frac{\alpha_{\text{dr}}}{\alpha_{\text{dr}} - 3w_{\text{dr}}} \rho_{\text{dm},0} a^{-3} (a^{-3w_{\text{dr}}} - a^{-\alpha_{\text{dr}}}), \quad (2.5)$$

where the subscript 0 denotes values today. For  $w_{\text{dr}} = 1/3$ , Eq. (2.5) can be further simplified to

$$\rho_{\text{dr}} = \beta a^{-4} + \frac{\alpha_{\text{dr}}}{1 - \alpha_{\text{dr}}} \rho_{\text{dm},0} a^{-(3+\alpha_{\text{dr}})}, \quad (2.6)$$

where  $\beta$  is a constant. The first term in Eq. (2.6) behaves like a standard radiation density while the second behaves like a fluid with an equation of state  $\alpha_{\text{dr}}/3$ . For weak couplings between dark matter and dark radiation,  $\alpha_{\text{dr}} \ll 1$  which leads to  $\beta \sim 0$ . Moreover, the first term redshifts faster than the second, always being subdominant. Hence, in our analysis, we only retain the second term. With this assumption, we obtain the fraction  $f_{\text{dm}}$  of dark matter that decays into dark radiation

$$f_{\text{dm}} = \frac{\rho_{\text{dr}}}{\rho_{\text{dm}}} \rightarrow \frac{\alpha_{\text{dr}}}{3w_{\text{dr}} - \alpha_{\text{dr}}} = \frac{\alpha_{\text{dr}}}{1 - \alpha_{\text{dr}}} \simeq \alpha_{\text{dr}}. \quad (2.7)$$

Therefore,  $f_{\text{dm}}$  is approximately constant over time and the density of dark radiation  $\rho_{\text{dr}} \simeq \alpha_{\text{dr}} \rho_{\text{dm}}$ . Our model is then parameterised by a single parameter  $\alpha_{\text{dr}}$ .

For a detailed description of the perturbations in our model, we refer the reader to Ref. [32, 41].

## 2.2 Calculation of $\Delta N_{\text{eff}}$

In standard cosmology, the energy density  $\rho_{\text{rad}}$  of relativistic species in terms of the photon energy density  $\rho_{\gamma}$  is

$$\rho_{\text{rad}} = \left[ 1 + \frac{7}{8} N_{\text{eff}} \left( \frac{4}{11} \right)^{4/3} \right] \rho_{\gamma}. \quad (2.8)$$

This includes standard model (SM) neutrinos (for which  $N_{\nu, \text{eff}} = 3.046$ ) [42, 43], and characterizes any free-streaming radiation beyond the SM expectation. Then, any departure from the SM can be accounted for through  $\Delta N_{\text{eff}}$ , where  $N_{\text{eff}} = N_{\nu, \text{eff}} + \Delta N_{\text{eff}}$ . In our case,  $\Delta N_{\text{eff}, \text{dr}}$  can be expressed in terms of  $\alpha_{\text{dr}}$  [32] as

$$\frac{7}{8} \Delta N_{\text{eff}, \text{dr}} \left( \frac{4}{11} \right)^{4/3} \frac{\rho_{\gamma,0}}{a^4} = \frac{1}{1 - \alpha_{\text{dr}}} \rho_{\text{dm},0} a^{-(3+\alpha_{\text{dr}})} - \rho_{\text{dm},0} a^{-3}, \quad (2.9)$$

making it a derived parameter in our analysis.

## 2.3 Effects on observables

The main effect of the DDM model is an alteration of the expansion history of the Universe. In Fig. 1, we show how decaying dark matter affects the CMB, the matter power spectrum and the expansion rate. All parameters were fixed at their Planck 2015  $\Lambda$ CDM best-fit values, including the energy density  $\Omega_{\text{dm},0}$  of dark matter today, and we show the effect of varying just  $\alpha_{\text{dr}}$ . Then, for  $\alpha_{\text{dr}} > 0$ , there was more dark matter in the early universe which decayed to match the dark matter energy density today. This shifts matter-radiation equality to earlier times, reduces the ratio  $\Omega_{\text{b}}/\Omega_{\text{dm}}$  of baryons to dark matter in the early universe and elongates the matter-dominated epoch of the Universe.

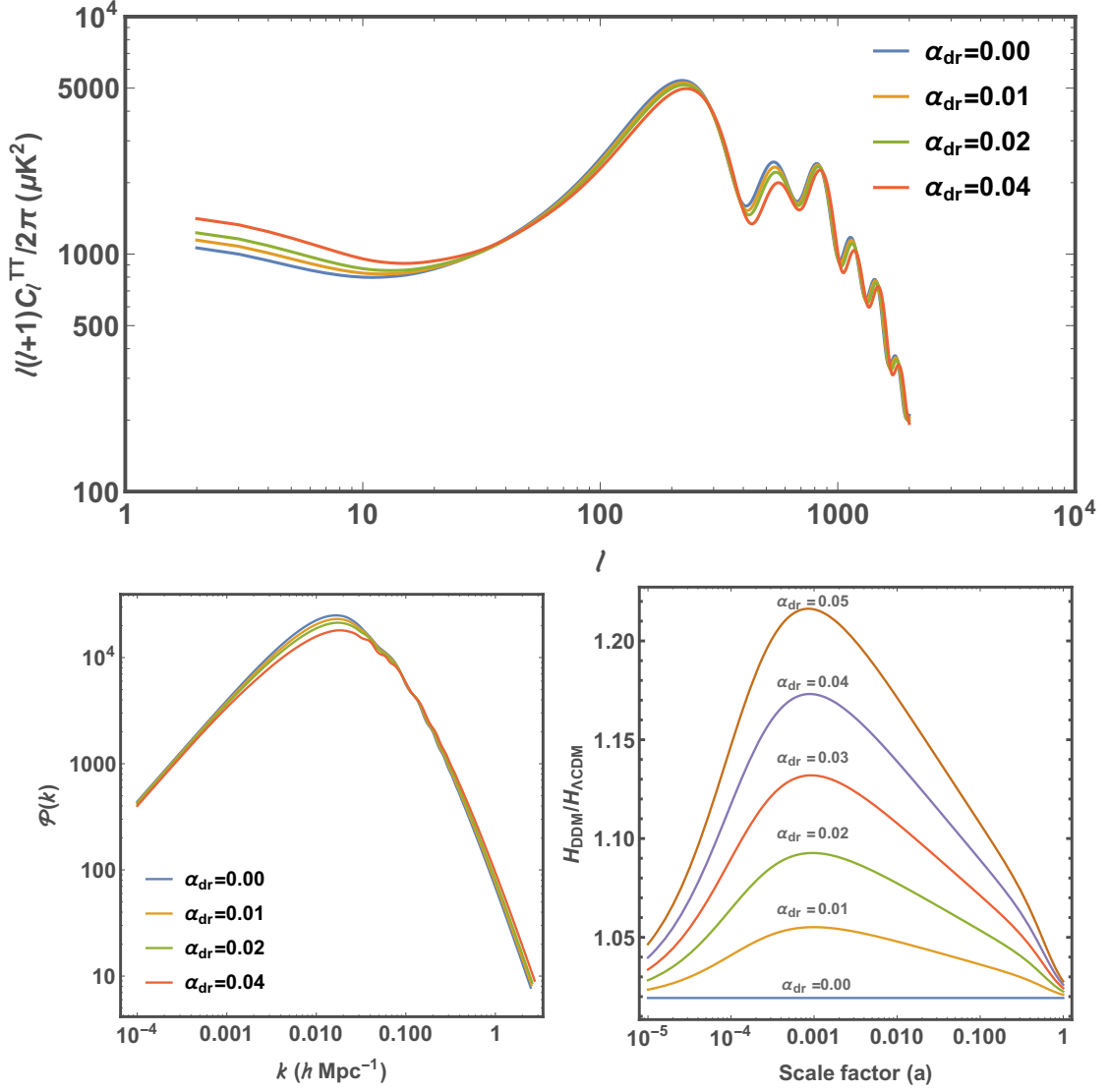


**Figure 1.** Shown here are the effects of DDM on various observables. These plots were produced using a modified version of CAMB, fixing all  $\Lambda$ CDM parameters, including  $\Omega_{\text{dm},0}$  and varying just  $\alpha_{\text{dr}}$ . The blue line with  $\alpha_{\text{dr}} = 0$  represents a  $\Lambda$ CDM cosmology. *Top*: effect of non-zero  $\alpha_{\text{dr}}$  on the CMB TT power spectrum; *left*: effect on the matter power spectrum; *right*: the DDM expansion rate relative to  $\Lambda$ CDM.

The bottom-right panel of Fig. 1 can then be understood as follows. At early times, the Universe is radiation-dominated and the Hubble rate  $H$  is given by

$$3H^2 M_{\text{Pl}}^2 = \left[ 1 + \frac{7}{8} N_{\nu, \text{eff}} \left( \frac{4}{11} \right)^{4/3} \right] \rho_\gamma + \frac{1}{1 - \alpha_{\text{dr}}} \rho_{\text{dm},0} a^{-(3+\alpha_{\text{dr}})} + \rho_{\text{b},0} a^{-3}. \quad (2.10)$$

Here,  $M_{\text{Pl}}$  is the reduced Planck mass and  $\rho_{\text{b},0}$  is the baryon density today. The dark radiation added by the DDM model is always subdominant, and the very early universe resembles a  $\Lambda$ CDM universe. As we approach matter domination, due to the extra dark matter in the Universe, the expansion rate increases, reaching a peak deviation close to  $z \sim 10^3$ . Finally, as the extra dark matter decays into

dark radiation which quickly redshifts away, the expansion rate relaxes back into agreement with  $\Lambda$ CDM. This effect is more pronounced as  $\alpha_{\text{dr}}$  increases. Overall, the expansion rate is increased in the DDM scenario relative to  $\Lambda$ CDM, the maximum increase occurring close to recombination. This combined with extra dark matter in the early universe shifts matter-radiation equality as well as recombination to earlier. If recombination occurs earlier, sound waves in the early universe have less time to travel, decreasing the sound horizon  $r_s$ . The Hubble parameter can then increase to compensate allowing the DDM model to diminish the Hubble tension.

These effects can also be inferred from the top panel of Fig. 1 showing the change in the CMB TT power spectrum. An increase in the amount of dark matter in the early universe suppresses power in all CMB peaks, as the enhancement due to acoustic driving is reduced. A smaller sound horizon shifts peak locations to smaller scales, or larger multipoles  $\ell$ . The effect of the reduced ratio  $\Omega_b/\Omega_{\text{dm}}$  is most apparent in the second peak. The heights of odd and even CMB peaks determine  $\Omega_b/\Omega_{\text{dm}}$ , with a smaller ratio implying a larger difference in peak heights [44]. Finally, power at large scales ( $\ell \lesssim 30$ ) is enhanced because dark matter decaying into dark radiation causes gravitational potential wells to decay, boosting the late integrated Sachs-Wolfe (ISW) effect.

Similar effects can also be seen in the matter power spectrum shown in the bottom-left panel of Fig. 1. The location of the peak in the matter power spectrum is dictated by the size of the Universe at matter-radiation equality, which the DDM model shifts to smaller sizes, or larger wavenumbers  $k_{\text{eq}}$  [45]. The enhancement of power at small scales is a result of the decrease in  $\Omega_b/\Omega_{\text{dm}}$ , which leads to less photon drag and boosts structure formation. On the other hand, large-scale modes enter the horizon in the late universe which has less dark matter than the early universe, but is still expanding faster than  $\Lambda$ CDM as seen from Fig. 1. This suppresses structure formation and therefore power at large scales. In particular, at scales  $\sim 8\text{Mpc}$ , power is considerably suppressed, alleviating the  $S_8$  tension. This suppression can also be attributed to DDM causing gravitational potential wells to decay, becoming shallower in the late universe. Moreover, as DDM dilutes as  $a^{-(3+\alpha)}$ , it is no longer pressureless and this pressure resists the growth of gravitational potential wells.

### 3 Methodology

To investigate this DDM model, we use a modified version of the publicly available Boltzmann code CAMB [46]. The modified version is based on the dynamics described in [32]; We vary the 6 standard  $\Lambda$ CDM parameters: the baryon density  $\omega_b$  today, the dark matter density  $\omega_{\text{dm}}$  today, the angular size  $\theta_{\text{MC}}$  of the sound horizon at recombination, the optical depth  $\tau$  to reionisation, the scalar spectral index  $n_s$ , and the amplitude  $A_s$  of the primordial power spectrum. To this, we add the DDM parameter  $\alpha_{\text{dr}}$ . We then use the publicly available Markov chain Monte Carlo code COSMOMC [47, 48] to explore our 7-dimensional parameter space with the following assumptions. We assume a flat universe with  $\Omega_k = 0$ , and a constant dark energy equation of state,  $w_{\text{de}} = -1$ . We also fix the running of the scalar spectral index  $dn_s/d\ln k = 0$  and the amplitude  $A_{\text{lens}} = 1$  of the lensing power spectrum. We adopt standard values for the sum of neutrino masses  $\Sigma m_\nu = 0.06$  eV and the SM  $N_{\nu, \text{eff}} = 3.046$ . The entire DDM model is described by the sole parameter  $\alpha_{\text{dr}}$ . The dark radiation energy density  $\Omega_{\text{dr}}$  and  $\Delta N_{\text{eff, dr}}$  are derived parameters which can be expressed in terms of  $\alpha_{\text{dr}}$ . Table 1 shows the priors for the 7 varied parameters.

We fit to various early and late-universe data sets in certain combinations. Our data include:

- **Planck** : The CMB temperature and polarization angular power spectra (high- $\ell$  TT + low- $\ell$  TEB) released by Planck 2015 [33, 49]

- **JLA** : Luminosity distance of supernovae Type Ia coming from ‘joint light-curve analysis’ using SNLS (Supernova Legacy Survey) and SDSS (Sloan Digital Sky Survey) catalogs [50]
- **BAO** : The ‘Baryonic Acoustic Oscillation’ data from DR12-BAO [51], SDSS-6DF [52] and SDSS-MGS [53]
- **R18** : An external gaussian prior on  $H_0 = 73.52 \pm 1.62$  km/s/Mpc [8].

We fit to the combinations Planck, Planck+R18 and Planck+JLA+BAO+R18. We adhere to the Gelman-Rubin convergence criteria of  $R - 1 < 0.01$  and discard the first 30% of our chains as burn-in.

Parameter	$\Lambda$ CDM	DDM
$\Omega_b h^2$	[ 0.005 , 0.1 ]	[ 0.005 , 0.1 ]
$\Omega_{dm} h^2$	[ 0.001 , 0.99 ]	[ 0.001 , 0.99 ]
$100\theta_{MC}$	[ 0.5 , 10 ]	[ 0.5 , 10 ]
$\tau$	[ 0.01 , 0.8 ]	[ 0.01 , 0.8 ]
$n_s$	[ 0.8 , 1.2 ]	[ 0.8 , 1.2 ]
$\ln(10^{10} A_s)$	[ 2.0 , 4.0 ]	[ 2.0 , 4.0 ]
$\alpha_{dr}$	–	[ 0.00 , 0.05 ]

**Table 1.** Priors on the cosmological parameters we vary in our MCMC analyses

## 4 Results

Figures 2-4 compare our posteriors for the  $\Lambda$ CDM (blue) and DDM (red) models for various data sets. Along with posteriors for  $\Omega_b h^2$ ,  $\Omega_{dm} h^2$  and  $\alpha_{dr}$ , we also show posteriors for the derived parameters  $H_0$  and  $S_8$ . The green bands represent local measurements of  $H_0$  and  $S_8$ . From these figures, the correlation of  $H_0$  with  $\alpha_{dr}$  and the anticorrelation of  $S_8$  with  $\alpha_{dr}$  are apparent. An increase in  $\alpha_{dr}$  results in a greater  $H_0$  and a smaller  $S_8$ . This is the exact effect required to solve the  $H_0$  and  $S_8$  tensions simultaneously. These correlations are most evident in the posteriors of Planck+R18 in Fig. 3. The inclusion of BAO data diminishes these correlations as seen in Fig. 4.

As seen from Fig. 2, Planck data places an upper bound on  $\alpha_{dr}$  ( $\leq 0.003$ ). However, the addition of an external prior on  $H_0$  from R18 leads to a small preference for non-zero  $\alpha_{dr}$  ( $\approx 0.005 \pm 0.003$ ) at the  $\sim 1.5\sigma$  level. With Planck+R18, the Hubble tension is reduced to  $\sim 1.5\sigma$  and the  $S_8$  tension to  $\sim 0.3\sigma$ . The addition of BAO data weakens these resolutions, as seen from Table 2. For Planck+JLA+BAO+R18, the  $H_0$  and  $S_8$  tensions remain at  $\sim 2.5\sigma$  and  $\sim 1.5\sigma$  levels respectively. For all dataset combinations explored, we remain consistent with  $\Lambda$ CDM within  $1\sigma$  for all  $\Lambda$ CDM parameters.

Table 3 shows the best-fit  $\chi^2$  values for the  $\Lambda$ CDM and DDM models. The DDM model leads to a slight improvement in fit, largely due to fitting the R18 measurement better than  $\Lambda$ CDM.

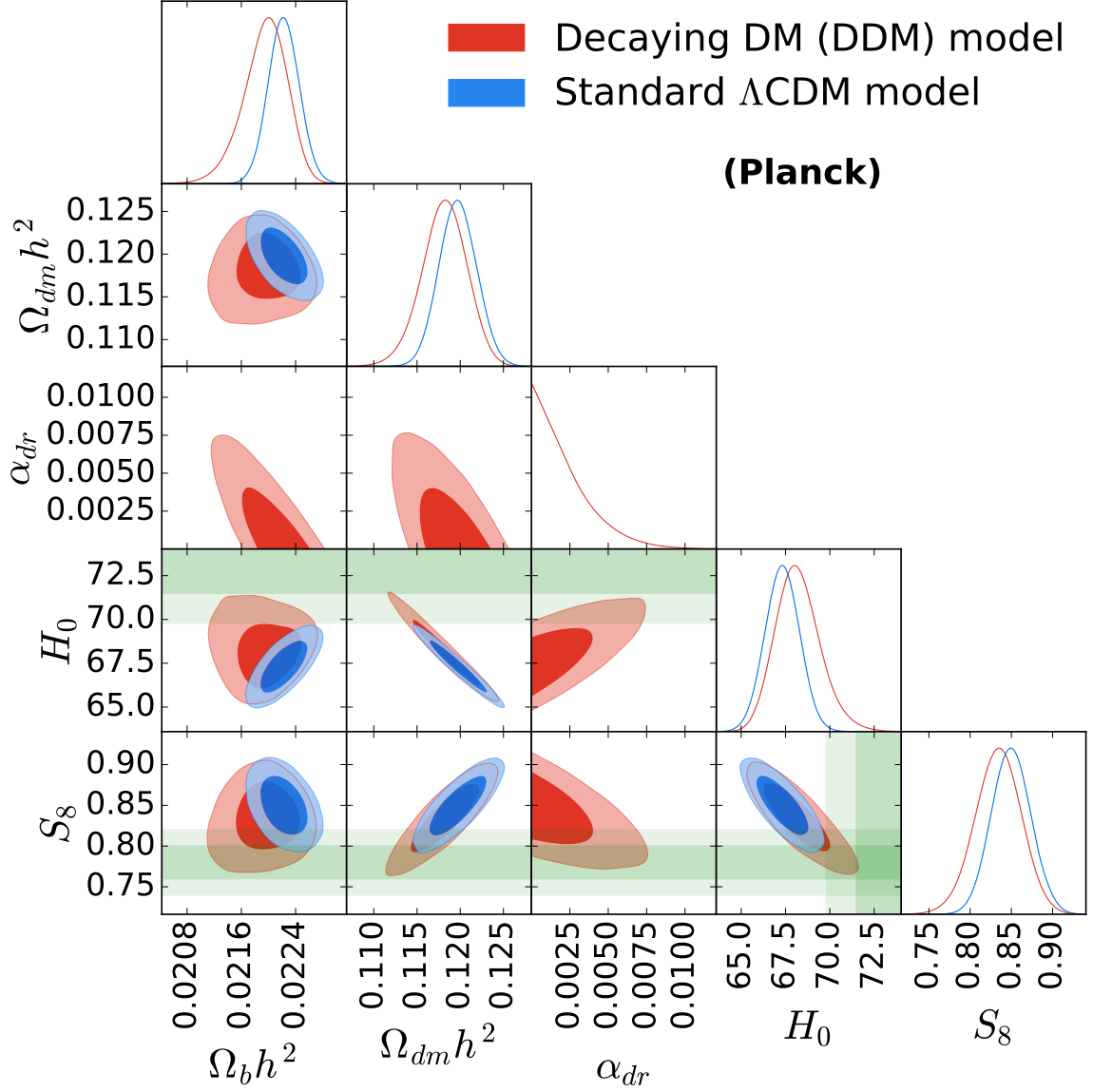


**Figure 2.** Comparison between the standard  $\Lambda$ CDM and the DDM models: Constraints on various cosmological parameters along with their covariances when tested against the Planck data. The green bands represent the constraints on  $H_0$  and  $S_8$  coming from [8, R18] and [12, DES-YI, 2017].

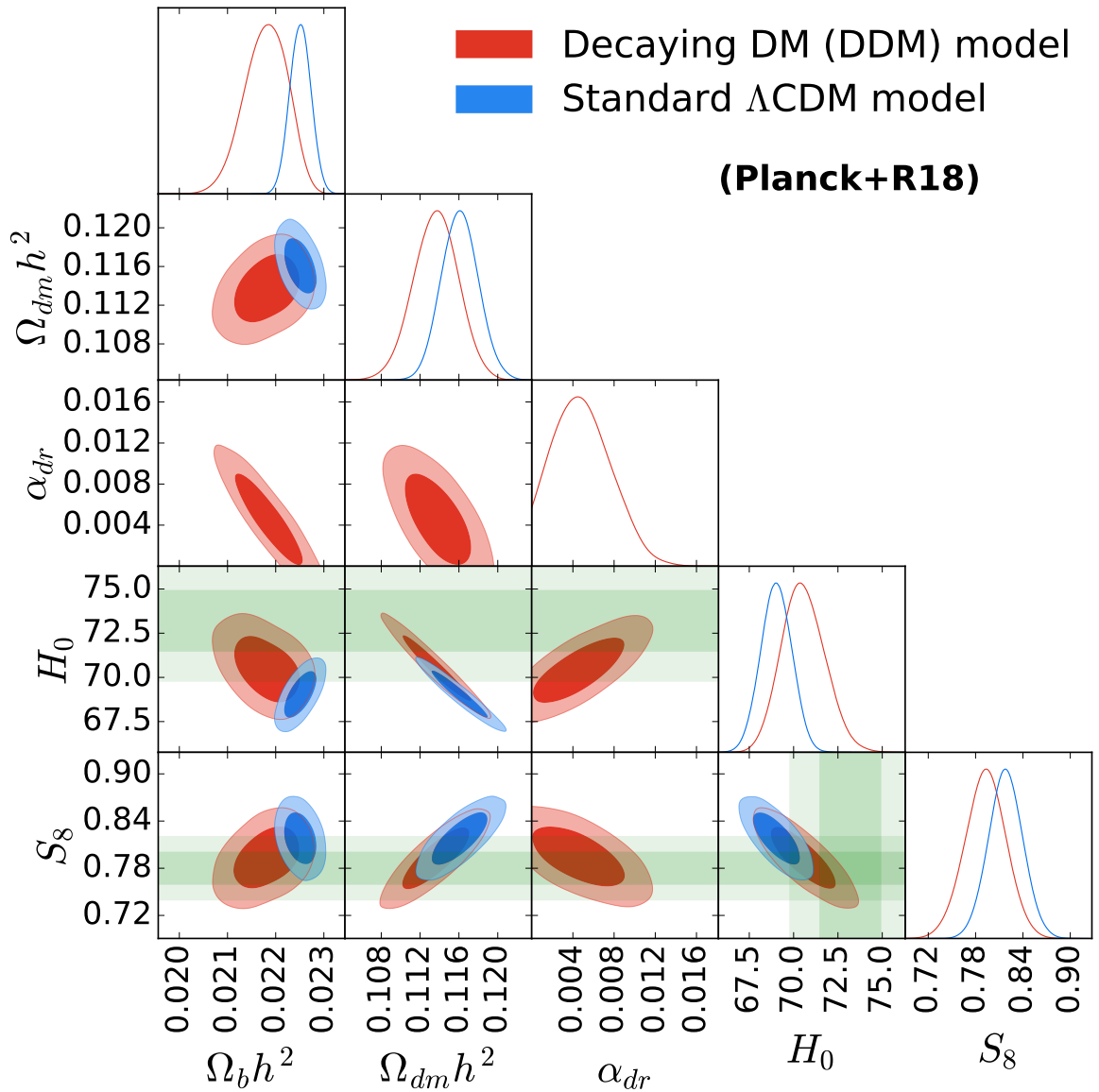


**Figure 3.** Comparison between the standard  $\Lambda$ CDM and the DDM models: Constraints on various cosmological parameters along with their covariances when tested against the Planck+R18. The green bands represent the constraints on  $H_0$  and  $S_8$  coming from [8, R18] and [12, DES-YI, 2017].

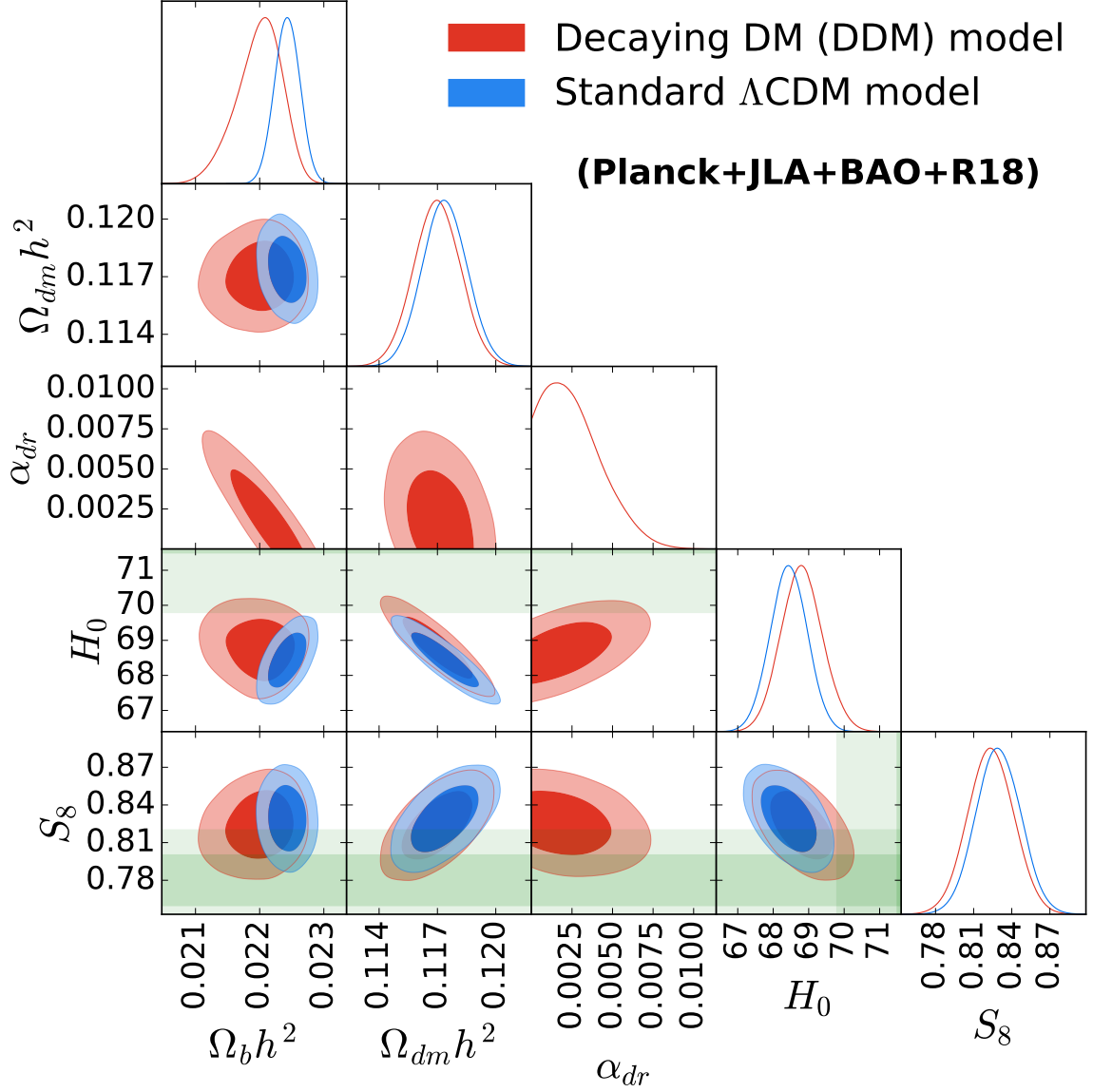


**Figure 4.** Comparison between the standard  $\Lambda$ CDM and the DDM models: Constraints on various cosmological parameters along with their covariances when tested against the Planck+JLA+BAO+R18. The green bands represent the constraints on  $H_0$  and  $S_8$  coming from [8, R18] and [12, DES-YI, 2017].

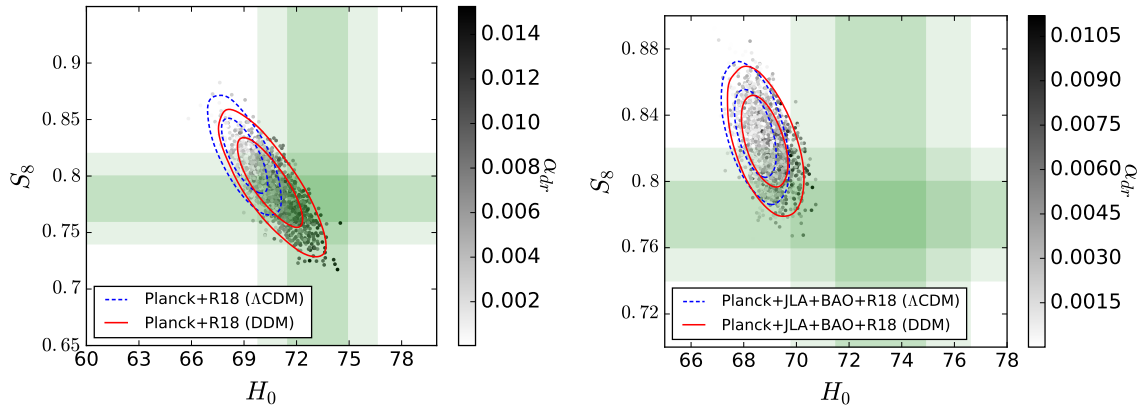


**Figure 5.** The figures show the  $\Lambda$ CDM (blue) and DDM (red) constraints on the  $H_0 - S_8$  plane for two dataset combinations, Planck+R18 and Planck+R18+JLA+BAO. The green bands represent the  $1$  and  $2\sigma$  constraints on  $H_0$  and  $S_8$  coming from [8, R18] and [12, DES-YI, 2017]. The scattered points are for the DDM model representing values of  $\alpha_{\text{dr}}$ .

In Fig. 5, we show how the decay parameter  $\alpha_{\text{dr}}$  improves the  $H_0$  and  $S_8$  tensions. In the DDM scenario (red contours),  $\alpha_{\text{dr}}$  increases towards the bottom right. Considering just Planck+R18, the external prior on  $H_0$  pushes the decay rate of dark matter to be  $\sim 1\%$  of the Hubble rate. These large values of  $\alpha_{\text{dr}}$  alter expansion history enough for the model to predict a larger  $H_0$  and suppress structure formation enough to predict smaller  $S_8$ . Without data at intermediate redshifts, such large changes in cosmology are permitted. As seen from the left panel of Fig. 5, within the scope allowed by Planck+R18, the DDM contours intersect the  $1\sigma$  local-measurement square (green). For these datasets, while the  $1\sigma$   $\Lambda$ CDM contour (blue) intersects the  $1\sigma$  local measurement of  $S_8$ , the  $2\sigma$   $\Lambda$ CDM contour is beyond the  $1\sigma$  local  $H_0$  measurement. Therefore, the DDM model diminishes the  $H_0$  and  $S_8$  tensions.

Including data at intermediate redshifts, namely JLA and BAO, the tensions remain unresolved. As seen from the right panel of Fig. 5, while DDM reduces the  $S_8$  tension to the  $1\sigma$  level, the Hubble tension still exists at the  $2.5\sigma$  level. The combined datasets Planck+R18+JLA+BAO do not permit large deviations from  $\Lambda$ CDM cosmology. Moreover, smaller values of  $\alpha_{\text{dr}}$  are permitted, with the decay rate of dark matter constrained to be  $\sim 0.5\%$  of the Hubble rate.

Parameter	Planck+R18		Planck+JLA+BAO+R18	
	$\Lambda$ CDM	DDM	$\Lambda$ CDM	DDM
$\Omega_b h^2$	$0.02251 \pm 0.00022$	$0.02180^{+0.00049}_{-0.00041}$	$0.02243 \pm 0.00020$	$0.02199^{+0.00041}_{-0.00029}$
$\Omega_{dm} h^2$	$0.1161 \pm 0.0019$	$0.1136 \pm 0.0023$	$0.1174 \pm 0.0012$	$0.1170 \pm 0.0012$
$100\theta_{MC}$	$1.04138 \pm 0.00045$	$1.04118 \pm 0.00045$	$1.04123 \pm 0.00041$	$1.04098 \pm 0.00044$
$\tau$	$0.094 \pm 0.019$	$0.089 \pm 0.020$	$0.089 \pm 0.018$	$0.082 \pm 0.019$
$\ln(10^{10} A_s)$	$3.113 \pm 0.037$	$3.107 \pm 0.038$	$3.106 \pm 0.035$	$3.096 \pm 0.037$
$n_s$	$0.9748 \pm 0.0058$	$0.9763 \pm 0.0058$	$0.9715 \pm 0.0043$	$0.9699 \pm 0.0044$
$\alpha_{dr}$	--	$0.0050^{+0.0023}_{-0.0034}$	--	$< 0.00332$
$\Omega_m$	$0.293 \pm 0.011$	$0.274 \pm 0.014$	$0.3000 \pm 0.0067$	$0.2950 \pm 0.0074$
$\Omega_\Lambda$	$0.707^{+0.012}_{-0.010}$	$0.725 \pm 0.014$	$0.7000 \pm 0.0067$	$0.7044 \pm 0.0073$
$\sigma_8$	$0.829 \pm 0.015$	$0.830 \pm 0.015$	$0.830 \pm 0.015$	$0.831 \pm 0.015$
$S_8$	$0.818 \pm 0.022$	$0.793 \pm 0.026$	$0.829 \pm 0.018$	$0.823 \pm 0.018$
$H_0$	$69.03 \pm 0.87$	$70.6^{+1.1}_{-1.3}$	$68.44 \pm 0.52$	$68.81 \pm 0.58$

**Table 2.** Comparison between the standard  $\Lambda$ CDM and the DDM models showing  $1\sigma$  constraints on parameters fitting to Planck+R18 and Planck+JLA+BAO+R18

Dataset	Plank+R18		Plank+JLA+BAO+R18	
	$\Lambda$ CDM	DDM	$\Lambda$ CDM	DDM
$\chi^2_{\text{high}\ell\text{TT}}$	768.352	771.684	767.395	767.154
$\chi^2_{\text{lowTEB}}$	10498.3	10496.5	10497.3	10497.9
$\chi^2_{\text{JLA}}$	--	--	695.377	695.299
$\chi^2_{6\text{DF}}$	--	--	0.0402244	0.0793526
$\chi^2_{\text{MGS}}$	--	--	2.34994	2.67358
$\chi^2_{\text{DR12BAO}}$	--	--	3.57457	3.96993
$\chi^2_{\text{nuisance}}$	1.50061	3.20412	3.11594	2.42671
$\chi^2_{\text{R18}}$	7.59589	2.46971	9.11007	7.98282
$\sum \chi_i^2$	11275.7	11273.8	11978.3	11977.5
$\Delta(\sum \chi_i^2)$	0	-1.9	0	-0.8

**Table 3.** Comparison between the standard  $\Lambda$ CDM and the DDM models:  $\chi^2$  values for various datasets from a combined fit to Planck+R18 and Planck+JLA+BAO+R18 are given, with the  $\chi^2_{\text{nuisance}}$  for expectations for the nuisance and foreground parameters.

## 5 Discussion and conclusions

While the  $\Lambda$ CDM model of cosmology fits numerous datasets well, its predictions based on the early and late universe disagree [4, 31]. The current expansion rate  $H_0$  is underpredicted by  $\Lambda$ CDM when fit to the early universe [7, 8]. Despite this, measurements of the late universe are in agreement with a  $\Lambda$ CDM expansion history, but with different parameter values [2]. This Hubble tension has persisted and worsened over the years and no systematic cause has yet been found [5]. Moreover,  $\Lambda$ CDM overpredicts the amplitude of matter fluctuations  $S_8$  relative to direct measurements in the late universe [6, 10]. Although this is a milder tension, combined, these tensions might hint new physics beyond the standard model of cosmology.

Theories that address each tension often worsen the other. In this paper, we explored a decaying dark matter model than can simultaneously improve both tensions. We considered dark matter that decays into dark radiation, parameterised by a single new parameter [32, 35]. The DDM model increases the expansion rate relative to  $\Lambda$ CDM, with the largest effect being close to recombination. This leads to a reduced sound horizon, to compensate for which  $H_0$  increases, alleviating the Hubble tension. The DDM model also reduces the dark matter density in the late universe, suppressing structure formation and lowering the predicted value of  $S_8$ . Hence, it offers solutions to both tensions simultaneously.

Considering just data from the early and current universes, that is the Planck+R18 combination, we find that the Hubble tension is reduced below the  $1.5\sigma$  level and the  $S_8$  tension below  $0.5\sigma$ . DDM not only significantly diminishes both tensions, but also provides a slightly better fit to these datasets with  $\Delta\chi_{\text{tot}}^2 = -1.9$ , as seen from Table 3. However, including measurements of the Universe at intermediate redshifts with Planck+R18+JLA+BAO, we find that the DDM model is strongly constrained and the  $H_0$  and  $S_8$  tensions persist at the  $\sim 2.5\sigma$  and  $\sim 1.5\sigma$  levels respectively. The DDM model alters expansion history relative to  $\Lambda$ CDM all through matter domination, as shown in Fig. 1. As found by numerous models that aim to resolve the Hubble tension through modifications of the late universe, late-universe datasets such as BAO and JLA strongly constrain expansion history and keep such models from fully resolving the Hubble tension [7, 22–24]. In this case, the “new physics” we add is present not only in the early universe where it has maximal effect, but throughout cosmic history. Its presence in the late universe would spoil the fits to BAO and JLA, keeping it from diminishing the  $H_0$  and  $S_8$  tensions further. This can also be seen from the tilt of the  $H_0$  and  $S_8$  vs  $\alpha_{\text{dr}}$  contours in Figs. 3 and 4. Without BAO and JLA data,  $\alpha_{\text{dr}}$  has a stronger correlation with  $H_0$  and anticorrelation with  $S_8$  in Fig. 3. This relaxes when intermediate-redshift datasets are added as in Fig. 4, implying that the addition of BAO and JLA data weakens the effectiveness of DDM at resolving both tensions.

Numerous models of dark matter interacting within the dark sector have been explored [54–57]. In these models, the interaction is effective only up to a certain scale and negligible at larger scales. This produces a cut-off-like feature in the matter power spectrum at small scales, keeping the power in scales  $\sim 8\text{Mpc}$  the same as in  $\Lambda$ CDM. For decaying dark matter with a constant time-independent decay rate [27, 36], the constraints are driven by the change to the late ISW effect on the large-scale CMB data. To be consistent with it, the dark matter must decay very slowly which only allows a slight improvement in the  $S_8$  tension. The DDM model considered here circumvents this by having a smaller decay rate in the early universe around decoupling which then increases with time. Models which introduce a time-dependent dark-matter drag force due to dark radiation which also shut-off at late times [38] have similar effects.

The  $S_8$  and Hubble tensions are intriguing results in cosmology. They require careful investigation whether from a systematic or a new-physics perspective. Future data may shed further light

on whether these anomalies are hints of physics beyond the standard model of cosmology after all.

## Acknowledgments

We thank Marc Kamionkowski for his comments on the initial results of this work. SD and TK acknowledge the IUSSTF-JC-009-2016 award from the Indo-US Science & Technology Forum which supported the project and facilitated the authors visiting each other. TK also acknowledges support from the 2018 Johns Hopkins Discovery Award.

## References

- [1] Planck Collaboration, N. Aghanim, M. Ashdown, J. Aumont, C. Baccigalupi, M. Ballardini, A. J. Banday, R. B. Barreiro, N. Bartolo, S. Basak, and et al., “Planck intermediate results. XLVI. Reduction of large-scale systematic effects in HFI polarization maps and estimation of the reionization optical depth,” *A&A* **596** (Dec., 2016) A107, [arXiv:1605.02985](#).
- [2] A. G. Riess, L. M. Macri, S. L. Hoffmann, D. Scolnic, S. Casertano, A. V. Filippenko, B. E. Tucker, M. J. Reid, D. O. Jones, J. M. Silverman, R. Chornock, P. Challis, W. Yuan, P. J. Brown, and R. J. Foley, “A 2.4% Determination of the Local Value of the Hubble Constant,” *ApJ* **826** (July, 2016) 56, [arXiv:1604.01424](#).
- [3] M. Ata *et al.*, “The clustering of the SDSS-IV extended Baryon Oscillation Spectroscopic Survey DR14 quasar sample: first measurement of baryon acoustic oscillations between redshift 0.8 and 2.2,” *Mon. Not. Roy. Astron. Soc.* **473** no. 4, (2018) 4773–4794, [arXiv:1705.06373](#) [[astro-ph.CO](#)].
- [4] G. E. Addison, D. J. Watts, C. L. Bennett, M. Halpern, G. Hinshaw, and J. L. Weiland, “Elucidating  $\Lambda$ CDM: Impact of Baryon Acoustic Oscillation Measurements on the Hubble Constant Discrepancy,” *Astrophys. J.* **853** no. 2, (2018) 119, [arXiv:1707.06547](#) [[astro-ph.CO](#)].
- [5] W. L. Freedman, “Cosmology at a Crossroads,” *Nat. Astron.* **1** (2017) 0121, [arXiv:1706.02739](#) [[astro-ph.CO](#)].
- [6] R. A. Battye, T. Charnock, and A. Moss, “Tension between the power spectrum of density perturbations measured on large and small scales,” *Phys. Rev.* **D91** no. 10, (2015) 103508, [arXiv:1409.2769](#) [[astro-ph.CO](#)].
- [7] Planck Collaboration, N. Aghanim, Y. Akrami, M. Ashdown, J. Aumont, C. Baccigalupi, M. Ballardini, A. J. Banday, R. B. Barreiro, and et al., “Planck 2018 results. VI. Cosmological parameters,” *ArXiv e-prints* (July, 2018) [arXiv:1807.06209](#), [arXiv:1807.06209](#).
- [8] A. G. Riess, S. Casertano, W. Yuan, L. Macri, B. Bucciarelli, M. G. Lattanzi, J. W. MacKenty, J. B. Bowers, W. Zheng, A. V. Filippenko, C. Huang, and R. I. Anderson, “Milky Way Cepheid Standards for Measuring Cosmic Distances and Application to Gaia DR2: Implications for the Hubble Constant,” *ApJ* **861** (July, 2018) 126.
- [9] V. Bonvin, F. Courbin, S. H. Suyu, P. J. Marshall, C. E. Rusu, D. Sluse, M. Tewes, K. C. Wong, T. Collett, C. D. Fassnacht, T. Treu, M. W. Auger, S. Hilbert, L. V. E. Koopmans, G. Meylan, N. Rumbaugh, A. Sonnenfeld, and C. Spiniello, “H0LiCOW - V. New COSMOGRAIL time delays of HE 0435-1223:  $H_0$  to 3.8 per cent precision from strong lensing in a flat  $\Lambda$ CDM model,” *MNRAS* **465** (Mar., 2017) 4914–4930, [arXiv:1607.01790](#).
- [10] I. G. McCarthy, S. Bird, J. Schaye, J. Harnois-Deraps, A. S. Font, and L. Van Waerbeke, “The BAHAMAS project: the CMB-large-scale structure tension and the roles of massive neutrinos and galaxy formation,” *Mon. Not. Roy. Astron. Soc.* **476** no. 3, (2018) 2999–3030, [arXiv:1712.02411](#) [[astro-ph.CO](#)].
- [11] Planck Collaboration, P. A. R. Ade, N. Aghanim, C. Armitage-Caplan, M. Arnaud, M. Ashdown, F. Atrio-Barandela, J. Aumont, C. Baccigalupi, A. J. Banday, R. B. Barreiro, and et al., “Planck 2013

- results. XX. Cosmology from Sunyaev-Zeldovich cluster counts,” *A&A* **571** (Nov., 2014) A20, [arXiv:1303.5080 \[astro-ph.CO\]](#).
- [12] DES Collaboration, T. M. C. Abbott, F. B. Abdalla, A. Alarcon, J. Aleksić, S. Allam, S. Allen, A. Amara, J. Annis, J. Asorey, and et al., “Dark Energy Survey Year 1 Results: Cosmological Constraints from Galaxy Clustering and Weak Lensing,” *ArXiv e-prints* (Aug., 2017) arXiv:1708.01530, [arXiv:1708.01530](#).
- [13] G. Efstathiou, “H0 Revisited,” *Mon. Not. Roy. Astron. Soc.* **440** no. 2, (2014) 1138–1152, [arXiv:1311.3461 \[astro-ph.CO\]](#).
- [14] G. E. Addison, Y. Huang, D. J. Watts, C. L. Bennett, M. Halpern, G. Hinshaw, and J. L. Weiland, “Quantifying discordance in the 2015 Planck CMB spectrum,” *Astrophys. J.* **818** no. 2, (2016) 132, [arXiv:1511.00055 \[astro-ph.CO\]](#).
- [15] **Planck** Collaboration, N. Aghanim *et al.*, “Planck 2016 intermediate results. LI. Features in the cosmic microwave background temperature power spectrum and shifts in cosmological parameters,” [arXiv:1608.02487 \[astro-ph.CO\]](#).
- [16] T. Shanks, L. Hogarth, and N. Metcalfe, “GAIA Cepheid parallaxes and ‘Local Hole’ relieve  $H_0$  tension,” [arXiv:1810.02595 \[astro-ph.CO\]](#).
- [17] A. G. Riess, S. Casertano, D. Kenworthy, D. Scolnic, and L. Macri, “Seven Problems with the Claims Related to the Hubble Tension in arXiv:1810.02595,” [arXiv:1810.03526 \[astro-ph.CO\]](#).
- [18] J. Soltis, A. Farahi, D. Huterer, and C. M. Liberato, “Percent-Level Test of Isotropic Expansion Using Type Ia Supernovae,” [arXiv:1902.07189 \[astro-ph.CO\]](#).
- [19] V. Poulin, T. L. Smith, T. Karwal, and M. Kamionkowski, “Early Dark Energy Can Resolve The Hubble Tension,” *arXiv e-prints* (Nov., 2018) arXiv:1811.04083, [arXiv:1811.04083 \[astro-ph.CO\]](#).
- [20] T. Karwal and M. Kamionkowski, “Dark energy at early times, the Hubble parameter, and the string axiverse,” *Phys. Rev.* **D94** no. 10, (2016) 103523, [arXiv:1608.01309 \[astro-ph.CO\]](#).
- [21] A. Bhattacharyya, U. Alam, K. Lal Pandey, S. Das, and S. Pal, “Are  $H_0$  and  $\sigma_8$  tensions generic to present cosmological data?,” *ArXiv e-prints* (May, 2018) , [arXiv:1805.04716](#).
- [22] V. Poulin, K. K. Boddy, S. Bird, and M. Kamionkowski, “Implications of an extended dark energy cosmology with massive neutrinos for cosmological tensions,” *Phys. Rev. D* **97** (June, 2018) 123504, [arXiv:1803.02474 \[astro-ph.CO\]](#).
- [23] E. Di Valentino, A. Melchiorri, E. V. Linder, and J. Silk, “Constraining dark energy dynamics in extended parameter space,” *Phys. Rev. D* **96** no. 2, (July, 2017) 023523, [arXiv:1704.00762](#).
- [24] E. Di Valentino, A. Melchiorri, and J. Silk, “Reconciling Planck with the local value of  $H_0$  in extended parameter space,” *Physics Letters B* **761** (Oct., 2016) 242–246, [arXiv:1606.00634](#).
- [25] E. Di Valentino, A. Melchiorri, and J. Silk, “Beyond six parameters: Extending  $\Lambda$  CDM,” *Phys. Rev. D* **92** no. 12, (Dec., 2015) 121302, [arXiv:1507.06646](#).
- [26] K. Ichikawa, M. Kawasaki, K. Nakayama, M. Senami, and F. Takahashi, “Increasing the effective number of neutrinos with decaying particles,” *Journal of Cosmology and Astro-Particle Physics* **2007** (May, 2007) 008, [arXiv:hep-ph/0703034 \[hep-ph\]](#).
- [27] K. Enqvist, S. Nadathur, T. Sekiguchi, and T. Takahashi, “Decaying dark matter and the tension in  $\sigma_8$ ,” *JCAP* **1509** no. 09, (2015) 067, [arXiv:1505.05511 \[astro-ph.CO\]](#).
- [28] E. Di Valentino and S. Bridle, “Exploring the Tension between Current Cosmic Microwave Background and Cosmic Shear Data,” *Symmetry* **10** no. 11, (2018) 585.
- [29] J. L. Bernal, L. Verde, and A. G. Riess, “The trouble with  $H_0$ ,” *J. Cosmology Astropart. Phys.* **10** (Oct., 2016) 019, [arXiv:1607.05617](#).
- [30] J. Evslin, A. A. Sen, and Ruchika, “Price of shifting the Hubble constant,” *Phys. Rev.* **D97** no. 10, (2018) 103511, [arXiv:1711.01051 \[astro-ph.CO\]](#).

- [31] K. Aylor, M. Joy, L. Knox, M. Millea, S. Raghunathan, and W. L. K. Wu, “Sounds Discordant: Classical Distance Ladder &  $\Lambda$ CDM -based Determinations of the Cosmological Sound Horizon,” [arXiv:1811.00537 \[astro-ph.CO\]](#).
- [32] O. Eggers Bjaelde, S. Das, and A. Moss, “Origin of  $\Delta N_{eff}$  as a result of an interaction between dark radiation and dark matter,” *J. Cosmology Astropart. Phys.* **10** (Oct., 2012) 017, [arXiv:1205.0553](#).
- [33] Planck Collaboration, P. A. R. Ade, N. Aghanim, M. Arnaud, M. Ashdown, J. Aumont, C. Baccigalupi, A. J. Banday, R. B. Barreiro, J. G. Bartlett, and et al., “Planck 2015 results. XIII. Cosmological parameters,” *A&A* **594** (Sept., 2016) A13, [arXiv:1502.01589](#).
- [34] M. G. Aartsen, K. Abraham, M. Ackermann, J. Adams, J. A. Aguilar, M. Ahlers, M. Ahrens, D. Altmann, K. Andeen, T. Anderson, and IceCube Collaboration, “Searches for Sterile Neutrinos with the IceCube Detector,” *Phys. Rev. Lett.* **117** (Aug., 2016) 071801, [arXiv:1605.01990 \[hep-ex\]](#).
- [35] J. Väliiviita, E. Majerotto, and R. Maartens, “Large-scale instability in interacting dark energy and dark matter fluids,” *J. Cosmology Astropart. Phys.* **7** (July, 2008) 020, [arXiv:0804.0232](#).
- [36] V. Poulin, P. D. Serpico, and J. Lesgourgues, “A fresh look at linear cosmological constraints on a decaying dark matter component,” *JCAP* **1608** no. 08, (2016) 036, [arXiv:1606.02073 \[astro-ph.CO\]](#).
- [37] J. Lesgourgues, G. Marques-Tavares, and M. Schmaltz, “Evidence for dark matter interactions in cosmological precision data?,” *JCAP* **1602** no. 02, (2016) 037, [arXiv:1507.04351 \[astro-ph.CO\]](#).
- [38] M. A. Buen-Abad, M. Schmaltz, J. Lesgourgues, and T. Brinckmann, “Interacting Dark Sector and Precision Cosmology,” *JCAP* **1801** no. 01, (2018) 008, [arXiv:1708.09406 \[astro-ph.CO\]](#).
- [39] Z. Chacko, Y. Cui, S. Hong, T. Okui, and Y. Tsai, “Partially Acoustic Dark Matter, Interacting Dark Radiation, and Large Scale Structure,” *JHEP* **12** (2016) 108, [arXiv:1609.03569 \[astro-ph.CO\]](#).
- [40] T. Bringmann, F. Kahlhoefer, K. Schmidt-Hoberg, and P. Walia, “Converting nonrelativistic dark matter to radiation,” *Phys. Rev.* **D98** no. 2, (2018) 023543, [arXiv:1803.03644 \[astro-ph.CO\]](#).
- [41] M.-Y. Wang and A. R. Zentner, “Effects of Unstable Dark Matter on Large-Scale Structure and Constraints from Future Surveys,” *Phys. Rev.* **D85** (2012) 043514, [arXiv:1201.2426 \[astro-ph.CO\]](#).
- [42] G. Mangano, G. Miele, S. Pastor, T. Pinto, O. Pisanti, and P. D. Serpico, “Relic neutrino decoupling including flavour oscillations,” *Nuclear Physics B* **729** (Nov., 2005) 221–234, [hep-ph/0506164](#).
- [43] G. Mangano, G. Miele, S. Pastor, and M. Peloso, “A precision calculation of the effective number of cosmological neutrinos,” *Physics Letters B* **534** (May, 2002) 8–16, [astro-ph/01111408](#).
- [44] W. Hu, N. Sugiyama, and J. Silk, “The Physics of microwave background anisotropies,” *Nature* **386** (1997) 37–43, [arXiv:astro-ph/9604166 \[astro-ph\]](#).
- [45] J. Lesgourgues and S. Pastor, “Massive neutrinos and cosmology,” *Phys. Rept.* **429** (2006) 307–379, [arXiv:astro-ph/0603494 \[astro-ph\]](#).
- [46] A. Lewis, A. Challinor, and A. Lasenby, “Efficient Computation of Cosmic Microwave Background Anisotropies in Closed Friedmann-Robertson-Walker Models,” *ApJ* **538** (Aug, 2000) 473–476, [arXiv:astro-ph/9911177 \[astro-ph\]](#).
- [47] A. Lewis, “Efficient sampling of fast and slow cosmological parameters,” *Phys. Rev. D* **87** no. 10, (May, 2013) 103529, [arXiv:1304.4473 \[astro-ph.CO\]](#).
- [48] A. Lewis and S. Bridle, “Cosmological parameters from CMB and other data: A Monte Carlo approach,” *Phys. Rev. D* **66** no. 10, (Nov., 2002) 103511, [astro-ph/0205436](#).

- [49] Planck Collaboration, N. Aghanim, M. Arnaud, M. Ashdown, J. Aumont, C. Baccigalupi, A. J. Banday, R. B. Barreiro, J. G. Bartlett, N. Bartolo, and et al., “Planck 2015 results. XI. CMB power spectra, likelihoods, and robustness of parameters,” *A&A* **594** (Sept., 2016) A11, [arXiv:1507.02704](#).
- [50] M. Betoule, R. Kessler, J. Guy, J. Mosher, D. Hardin, R. Biswas, P. Astier, P. El-Hage, M. König, and et al., “Improved cosmological constraints from a joint analysis of the SDSS-II and SNLS supernova samples,” *A&A* **568** (Aug., 2014) A22, [arXiv:1401.4064](#).
- [51] S. Alam, M. Ata, S. Bailey, F. Beutler, D. Bizyaev, J. A. Blazek, A. S. Bolton, J. R. Brownstein, A. Burden, and et al., “The clustering of galaxies in the completed SDSS-III Baryon Oscillation Spectroscopic Survey: cosmological analysis of the DR12 galaxy sample,” *MNRAS* **470** (Sept., 2017) 2617–2652.
- [52] F. Beutler, C. Blake, M. Colless, D. H. Jones, L. Staveley-Smith, L. Campbell, Q. Parker, W. Saunders, and F. Watson, “The 6dF Galaxy Survey: baryon acoustic oscillations and the local Hubble constant,” *MNRAS* **416** (Oct., 2011) 3017–3032, [arXiv:1106.3366](#).
- [53] A. J. Ross, L. Samushia, C. Howlett, W. J. Percival, A. Burden, and M. Manera, “The clustering of the SDSS DR7 main Galaxy sample - I. A 4 per cent distance measure at  $z = 0.15$ ,” *MNRAS* **449** (May, 2015) 835–847, [arXiv:1409.3242](#).
- [54] P. Serra, F. Zalamea, A. Cooray, G. Mangano, and A. Melchiorri, “Constraints on neutrino – dark matter interactions from cosmic microwave background and large scale structure data,” *Phys. Rev.* **D81** (2010) 043507, [arXiv:0911.4411](#) [[astro-ph.CO](#)].
- [55] F.-Y. Cyr-Racine, R. de Putter, A. Raccanelli, and K. Sigurdson, “Constraints on Large-Scale Dark Acoustic Oscillations from Cosmology,” *Phys. Rev.* **D89** no. 6, (2014) 063517, [arXiv:1310.3278](#) [[astro-ph.CO](#)].
- [56] S. Das, R. Mondal, V. Rentala, and S. Suresh, “On dark matter - dark radiation interaction and cosmic reionization,” *JCAP* **1808** no. 08, (2018) 045, [arXiv:1712.03976](#) [[astro-ph.CO](#)].
- [57] R. J. Wilkinson, C. Boehm, and J. Lesgourgues, “Constraining Dark Matter-Neutrino Interactions using the CMB and Large-Scale Structure,” *JCAP* **1405** (2014) 011, [arXiv:1401.7597](#) [[astro-ph.CO](#)].